Optimisation of X-Ray CT within SPECT/CT Studies

By

Layal Jambi

Supervisors

Dr. Alan Britten, Anton Paramithas, Andy Irwin

A dissertation submitted to the Department of Physics, University of Surrey, in partial fulfilment of the degree of Master of Science in Medical Physics

Department of Physics

Faculty of Engineering & Physical Sciences

University of Surrey

September 2013

Declaration of Originality

I hereby confirm that I am the sole author of this theses project and is entirely my own work. The materials and information used or derived from other published or unpublished sources has been clearly sited and appropriately acknowledged and a list of references is given in the bibliography. I also declare that this thesis has not been submitted for a higher degree to any other University or institution.

In submitting this final version of my literature to the turnitin anti-plagiarism software resource, I certify that my work does not contravene the university regulations of plagiarism as described in the Student Handbook. I appreciate that if an allegation of plagiarism is upheld via an Academic Misconduct Hearing, then I may lose any credit for this module or a more severe penalty may be agreed.

Title: Optimisation of X-Ray CT within SPECT/CT Studies

Author: Layal Jambi

Author Signature Date: 09 Sep 2013

Supervisor's name:

Dr. Alan Britten, Anton Paramithas, Andy Irwin

Acknowledgement

I would never have been able to finish my dissertation without the help and support from my family and my friends.

I would like to express my deepest gratitude to my supervisors Dr. Alan Britten for his useful comments, remarks and guidance through the writing process of my master thesis. And for his continuous support and patience.

Also, I would like to thank Anton Paramithas for his useful advices, strong support and kindness also he introduced me to St Helier Hospital Staff and helped me in performing the experiment there and keep working with me late until night. And I would like to thank Andy Irwin.

In addition, I would like to appreciate Dr. Arum Parthipun, Consultant Radionuclide Radiologist for his time and his great cooperation in reading the images and many thanks to all the staff in the Nuclear Medicine Department at St. Helier Hospital.

Furthermore, I would also like to thank my mother and my father, my sisters and my brothers for their endless love. They were always supporting me and encouraging me with their best wishes.

Finally, my great compliment is to King Saud University, Riyadh, Saudi Arabia, and the Royal Embassy of Saudi Arabia Cultural Bureau in London for their financial support they provided for my MSc study.

Abstract

This dissertation introduces methods to optimise the X-ray CT exposures within SPECT/CT studies. In this project I correlate between the body mass index BMI and the CT dose exposed to patients. In this project SPECT/CT lumbar spine for facet joint had been chosen specifically. The experimental part was divided into two phases: phase l and phase ll. In phase l the phantom had been prepared and 12 different acquisitions had been acquired for both SPECT and CT with different CT parameters each time. In phase ll radioactive material Tc^{99m} had been administered into the facet joint. Also a source in a syringe inserted alongside the lumbar spine. Then 3 different acquisitions had been acquired for both SPECT and CT as well. A nuclear medicine radiologist evaluated the 15 acquired images qualitatively for localisation quality purposes. Assessment of the images concluded with determining the best and the worst images acquired. The best image acquired is the one with high kVp 130 and high mAs 60. In contrast, the worst image is the one acquired with low kVp 80 and low mAs 20. Then the images are evaluated according to the CT noise level in the image by measuring the SD, the larger the SD which is the one with 130 kVp 20 mAs the higher the image noise. Finally, this paper concludes with that all the findings are appropriate with the large patients since the phantom size best corresponds to larger patients.

Table of contents

Introduction

Nowadays, medical imaging technologies have combined together to perform what is called hybrid imaging. Single Photon Emission Computed Tomography combined with X-ray computed tomography (CT) is called SPECT/CT and is one of the modern modalities in nuclear medicine, which is providing X-ray exposures, and detecting gamma rays released from the radiopharmaceutical (Jacene, 2008). SPECT/CT has a particular property that is able to provide both functional and anatomical information from a single study. Dual advantages of anatomical localisation and attenuation correction could be achieved by the integration of CT with SPECT. Recently, radiologists and physicists focusing on the increased external radiation exposure dose which is X-ray from a CT device (Larkin, 2011). Besides, some of the SPECT investigations produce a high patient effective dose from the internal radiation exposure gamma γ-ray resulting from the administration of a radiopharmaceutical.

The main aim of the project is to develop methods to optimise and evaluate different approaches for X-ray CT exposures within SPECT/CT studies, which is concerning in minimizing patient's absorbed dose as low as reasonably achievable (ALARA) principle and maintaining the CT image quality in SPECT/CT to the best. Hence, the integration of CT with SPECT will allow co-registering of anatomical and molecular images, which is lead to attenuation correction accurately, and proper anatomical localisation of lesions with increased uptake that is to say low CT dose (Delbeke, 2009). Otherwise high CT dose could be used to increase image resolution in particular diagnostic quality. In this project the focus will be on the optimisation of CT dose in localisation only. In low dose CT the attenuation correction is generated by creation of attenuation correction maps, which are applied to the molecular image so that the differential absorption of radionuclide photons is corrected. If the attenuation map is incorrect, or contains too much statistical noise then it may provide imprecise radioactive distribution data leading to reduce the sensitivity and specificity of the final image. On the contrary, in high dose CT the diagnostic quality could be obtained as standard clinical CT with multi-slice CT detector which simultaneously generate a correlation between the high anatomical resolution and physiological image that means it gives the benefit for both localisation and diagnosis (Thompson et al. 2009). Some of the ways used to reduce CT dose are optimizing scanning parameters, Automatic exposure control (AEC) which is considered an effective technique for patient dose reduction and adaptive collimation to reduce effect of over scanning (McCollough et al. 2006).

The methodology of the project is firstly to investigate the correlation between the body mass index BMI and the patient's abdominal dimension. This is done by measuring the thickness of the patient from the CT image obtained from SPECT/CT studies. The main reason for doing that is to check the phantom, which will be used in the experiment, is of a reasonable size, since the problems of localisation and dose reduction are harder for larger patients. Moreover, the experimental part of the project will be accomplished by using an anthropomorphic phantom which is made of Perspex to determine the relationship between computed tomography dose index CTDI and image noise in the CT image and image noise in the attenuation corrected SPECT image. Facet joint SPECT localisation study have been chosen specifically to optimise the X-ray CT dose as SPECT is believed as the least diagnostic modality that has been used in a wide range of patients who suffer from spinal pain (Makki et al. 2010). Also, facet joint is considered an area of clinically interest at the department of nuclear medicine in St. Helier Hospital, as the experiment would be done there. In addition, the strong need for clear CT and SPECT is to localise for injection into the facet joint for pain relief. Furthermore, through the experiment the accuracy of the attenuation correction as a function of CTDI and CT image noise will also be investigated, particularly for low dose procedures on large patients where CT number accuracy is a known problem. It is not ethical to optimise any SPECT/CT protocol directly to patient, so optimisation of CT acquisition protocol had been studied to reduce patient dose by conducting a phantom study. Later, after completing the acquisitions a nuclear medicine radiologist qualitatively evaluated 15 images for localisation quality namely (image noise, spatial resolution and many other standards). Finally, challenges faced due to the restricted time of the project the patient study work will be limited to a few illustrative examples of how the method could be applied.

Chapter 1

Imaging System

1.1 Computed Tomography

Computed tomography (CT) is a radiological diagnostic procedure, which is used to investigate a wide range of disease states. CT is a cross sectional imaging technique uses X-rays that are producing a diagnostic radiology images with better insight into the pathogenesis of the body. In 1972, Godfrey Hounsfield developed the first CT method by using a commercial X-ray machine (David et al. 2006). It was possible for the first time to acquire non-superimposed images of an object slice by the aid of computed tomography.

Furthermore, today CT is considered one of the most significant modalities of radiological diagnostic imaging. CT creates non-superimposed, cross-sectional images of the body since much smaller contrast differences are evident in the CT image than conventional X-ray images. This allows the radiologists to visualize a specific and small difference structures in soft tissue regions for better image interpretation (Hsieh, 2013).

Moreover, there are four generations of CT scanners; the first generation which is the simplest type was invented in 1972 with a single X-ray beam and a single (1-D) detector. Then the second generation appeared in 1980 with a narrow fan beam X-ray and small area (2-D) detector. Next, the third generation was modified in 1985 with a wide-angle fan beam and a large area (2-D) detector. Finally, the fourth generation was developed in 1990 with a wide-angle rotated fan beam X-ray. After that, the fifth generation of CT has been discovered that is called electron beam. That generation considered as the fastest scanner, which emit electron beam to the anode target rotating around the patient to generate, X-rays (Pryor, 2013).

In 1991, the newest CT scanners are spiral or helical CT and the main concept of those scanners that the introduction of slip rings which allow continuous rotation of tubes and detectors on spiral or helix direction (Kopp et al. 2000). Following that in 1998, the latest advance has been introduced recently is the multi-slice CT (MSCT). It is a special type of CT scanners which data is collected simultaneously at different slice locations with a multiple row detector array (Hu, 1999).

1.2 Nuclear Medicine

Nuclear medicine is a physiological functional imaging procedure, which is considered as a branch of radiology that is based on administration of radioactive material that is called radiopharmaceutical in either diagnostic or therapeutic applications. The radiopharmaceutical can be obtained by integration of a radionuclide into a pharmaceutical. The main concept of nuclear medicine is to count the radioactivity presents inside the patient's body by observing the distribution behaviour of the administered pharmaceutical (Peter et al. 2005). This follows some physiological pathway, which aggregate in some parts of the body during a short period of time.

Furthermore, measurements of activity can be achieved either in vivo or in vitro. In vivo means that within the living organism to be investigated. In contrast, in vitro means ''within the glass'' which refers to measurements made by taking a sample material from patients. In 1957 the most common nuclear medicine imaging system was developed that is to say Gamma Camera, which is used to detect the gamma rays coming out from the patient's body (Maher et al. 2006).

1.3 Single Photon Emission Tomography

Fig. Dual headed Gamma Camera

In the late 1960s and early 1970s single photon emission computed tomography SPECT has been used clinically. The most significant importance of SPECT that it provides a three dimensional (3-D) distribution of radioactivity. That is to say to overcome the problem

that a 2-D image performs superimposed layers and structures without detailed information of the overlying and underlying organs. Commonly, there are three orthogonal planes which SPECT images can be shown: trans-axial, sagittal and coronal (Sharp et al. 2005). Therefore, to achieve that multiple projection views the camera heads are rotated mechanically around the patient at well-defined angles. SPECT is normally obtained with single photon gamma ray emitting radionuclides like Tc^{99m} and I^{131} that possess long half-life 6.06 hours and 8.01 days respectively (Powsner et al. 2006).

Chapter 2

SPECT/CT Studies

2.1 Body Mass Index

Objectives

The main aim of this section of the project is to find a correlation and evaluate the association between patient's weights and abdominal cross sectional dimensions and CTDI_{vol} dose in SPECT/CT studies. The reason why to do that is to check the phantom's size which will be used in the experiment whether it is of a reasonable size, owing to the problems of localisation and dose reduction are harder for larger patients.

Material and Methods

Patient's weight and height had been recorded just prior to the study. Then the body mass index BMI had been calculated according to the equation (eMED TV, 2013):

$$\text{BMI} = \frac{Weight\ (kg)}{Height\ (m) x\ Height\ (m)}$$

After that, the dimension of the cross sectional abdominal circumferences had been measured that is the thickness of the abdominal fat wall. Also, the CT dose parameters such as mAs, kVp and CTDI_{vol} had been recorded as well for any further considerations.

The first group studied was 9 patient's data that have bone scan study had been collected with different BMI who had been requested to do SPECT/CT at the pelvis area as an additional view at St. Helier Hospital (Appendix 1).

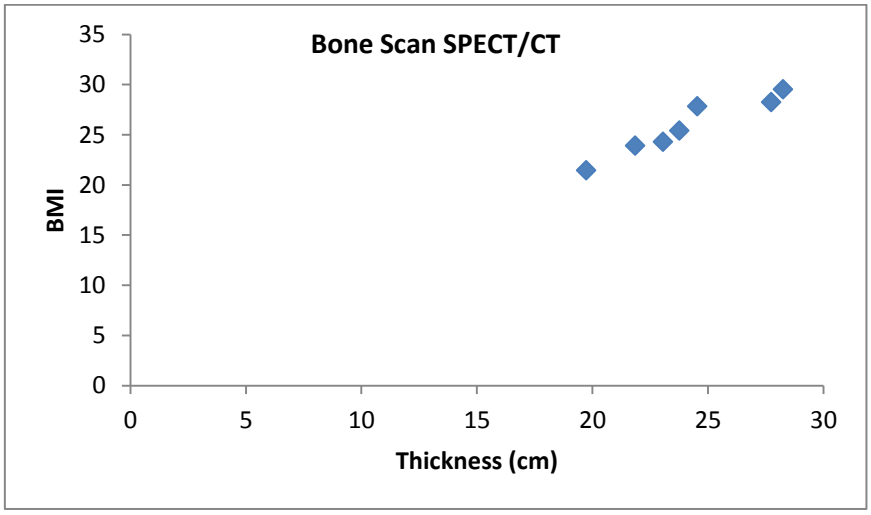

Graph 1: Thickness *vs* BMI in Bone SPECT/CT scan

While the next group studied was 9 Patient's data had been collected with different BMI who underwent stress-rest myocardial perfusion Imaging (MPI) single photon emission tomography SPECT as part of the main protocol at St. Helier Hospital (Appendix 2).

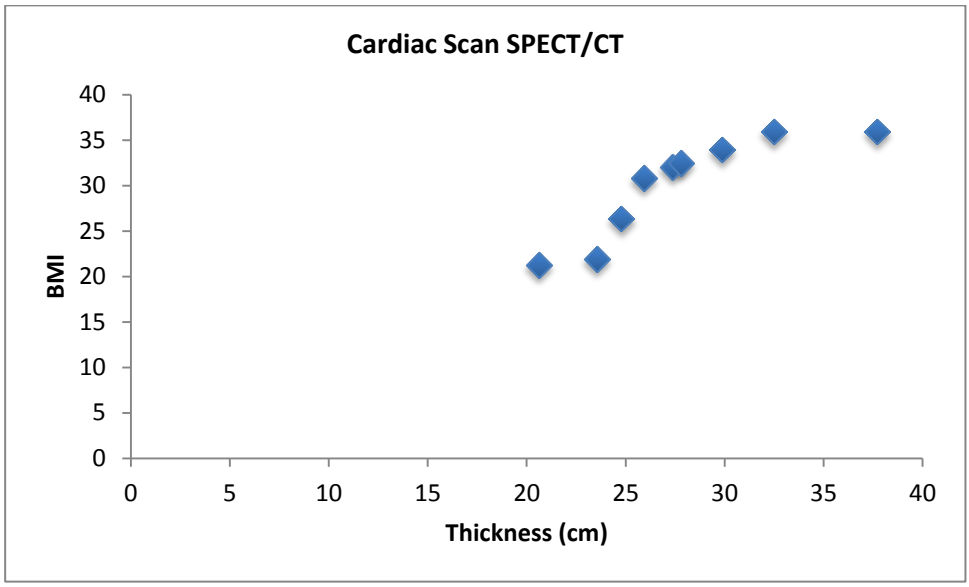

Graph 2: Thickness *vs* BMI in cardiac SPECT/CT scan

The specifications of the used phantom as given by the manufacturers (DSC, 2013):

Lateral outside dimensions	38 cm
Lateral inside dimensions	36 cm
Anterior posterior outside dimensions	26 cm
Anterior posterior inside dimensions	24 cm
Wall thickness	9.5 mm

By substituting the value of the anterior posterior outside dimension that is 26 in the equation derived from the graph we obtained the phantom's BMI, which is 28.33. The graphs below illustrate the relation between thickness versus BMI. And the value of the derived BMI has been plotted as well. That means our phantom is a quite large then in that case our optimisation should be applied to large patients.

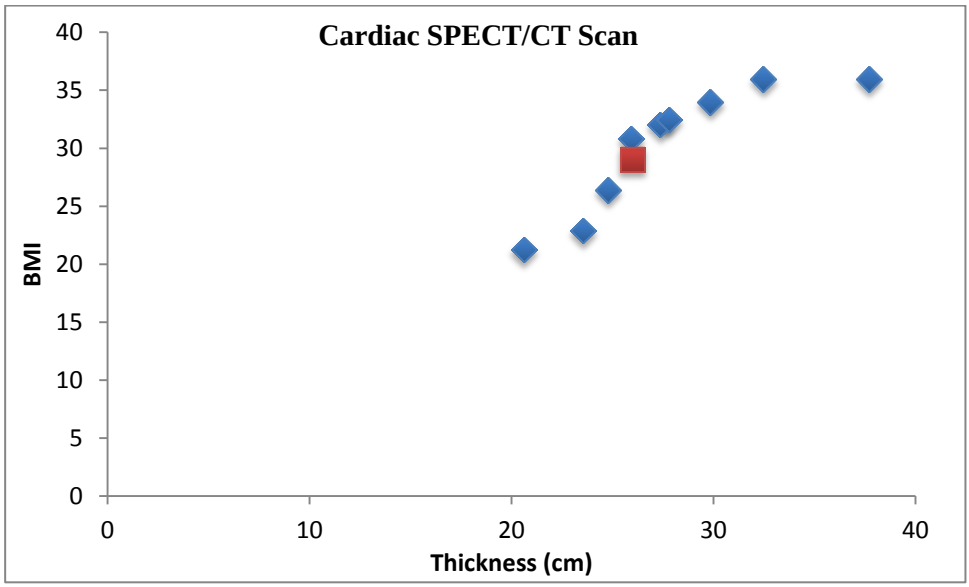

Graph 3: Correlation of phantom's size to calculate the corresponding BMI.

2.2 Facet Joint

It has been suggested that the lumbar facet joint (FJ) is the source of low back pain (LBP) (Schutz et al. 2011). SPECT and Bone Scintigraphy could be applied to evaluate and estimate the severity of the lower back pain, especially when a bone abnormality is suspected. Furthermore, administration of a radioactive material will identify and localize the affected bone joint. Hence, the distribution of the radionuclide activity will improve the visualisation of the vertebral bodies and the individual posterior element separately. As lumbar spine SPECT is a non-invasive procedure, the only risk associated with it is the increased radiation exposure (O'Neill et al. 2010).

It was decided to optimise the lumbar spine facet joint (FJ) study in this project, as it is an area of clinical interest at St. Helier Hospital. In FJ cases, metastasis is not expected to appear, as it is not the main concern. Radiologists only work with which level the facet joint are. The main interest is to see whether there is any uptake associated with FJ by CT. Also determine if it is in the right or left side. Usually, the uptake expected to be over the FJ on both sides. Besides in St. Helier Hospital they used the FJ study for localisation purposes only, which is our main objective of this project to optimise the CT dose within SPECT/CT for localisation purposes.

Chapter 3

Dosimetry Methodology

3.1 Radiation Risk Related to Medical Imaging

As the CT and Nuclear Medicine produce ionising radiation, which are X-rays and gamma rays respectively, they interact with the human body either directly or indirectly and cause damage to tissue cells. According to literatures CT and nuclear medicine are considered the most radiographic studies producing a high radiation dose (Soderberg, 2012). As a result, the radiation dose from medical examination could be estimated by measuring the effective dose. In fact the effective dose is theoretically calculated which is based on the multiplication of the organs exposed by the radiation applied by the tissue weighting factors in other words:

$$H_E = \sum_T H_T \; x \; W_T$$

Where H_E is the effective dose, H_T the equivalent dose and W_T tissue-weighting factor. Note H_E and H_T both have SI unit of Sieverts (SV) (Walker, 2013). However, the effective dose is generally used to estimate the level of radiation risk and not to determine the exact radiation dose from an imaging study (Eugene, 2010).

3.2 Nuclear Medicine Dosimetry

In nuclear medicine procedures, the fundamental measurable dose quantity is the administered radiopharmaceutical and patient's age. Therefore, the absorbed dose to a patient having SPECT scan is based on the physical properties of the radionuclide and biological behaviour of the administered activity (Soderberg, 2012). As the main concept of the radioactive material is to accumulate in some organs more than others, so that the absorbed dose can be measured in that organs in addition to the radiosensitive organs (Stabin et al., 1999).

3.3 CT Dosimetry

Determination of patient exposure to CT is slightly different than in conventional X-ray exposures. However, in CT the X-ray tube rotates all around the patient and producing

thin slices of the exposed body organs. When the X-rays penetrate the body's organ, some of the beam energy is absorbed by the organ. The International Commission on Radiation Units and Measurement (ICRU) defines the absorbed dose as the amount of energy imparted per unit mass at a point that is.

$$D = \frac{\Delta E_D}{\Delta m}$$

Where: D is the absorbed dose, ΔE_D energy deposited and Δm mass of matter. The SI unit for absorbed dose is gray (Gy) (Walker, 2013).

Then in that case, estimation of the effective absorbed CT dose in organs and tissues are related to two main quantities: CTDI computed tomography dose index and DLP dose length product DLP. Since 1980s the CTDI is the standard measure used to measure the CT radiation dose. The ideal CTDI for single axial scan in air is commonly $CTDI_{100}$. The $CTDI_{100}$ can be expressed by:

$$CTDI_{100} = \frac{1}{nT} \int_{-50\,mm}^{50\,mm} D(z)dz$$

Where *n* slice numbers, *T* slice thickness, *D(z)* dose profile along the axis of rotation (Kim et al., 2011). Weighted dose index $CTDI_w$ was introduced to calculate the absorbed dose for the (x, y) scan plane:

$$CTDI_W = \frac{1}{3}\, CTDI_{100\,(central)} + \frac{2}{3}\, CTDI_{100\,(Peripheral)}$$

Volume dose index $CTDI_{vol}$ was introduced in helical CT:

$$CTDI_{vol} = \frac{CTDI_W}{Pitch}$$

The unit of $CTDI_{vol}$ is mGy and the reading of its value represented on the CT consoles. $CTDI_{vol}$ defined as the exposure output measurements of the CT scanner (Soderberg, 2012).

While the DLP expression is account for measuring the overall transmitted energy within CT scan:

$$DLP = CTDI_{vol} \,.\, L$$

Where *L* scan length and DLP is measured in mGy.cm (Bongartz et al., 2004).

3.4 SPECT/CT Dosimetry

The recent combination of hybrid imaging SPECT with CT, multiple procedures can be done without moving the patient from one machine to another but just moving the position of the patient table to reach the field of view of the body region to be examined. Usually the CT image is used to produce the attenuation correction maps for SPECT image. On the other hand, the SPECT/CT patient undergoes a CT scan regardless of having a similar scan in a CT, alone which expose the patient to more doses. So to cope that issue, as the literature has studied "low dose CT is performed using thicker collimation and lower mAs. The low dose CT acquisition protocol dose not significantly affects attenuation correction and anatomic delineation in SPECT". Also, literature studies agree that the hybrid imaging system causes an obvious increase in patient radiation dose. In other words, the CT integration in nuclear medicine imaging system owing to a considerable increase of the total radiation dose exposed to patient. Despite the fact that SPECT/CT delivers more radiation to patient than SPECT alone, it has many advantages of introducing CT to patients. Therefore, introduction of CT radiation can be used in two main aims either diagnostic or localisation purposes by adjusting the CT parameters (Mhiri et al. 2012).

3.5 Exposure Parameters and CT Dose

In CT the most significant problem in figuring out exposure parameters is image noise and its effect on image quality. Some parameters influencing radiation exposure are: kVp, mAs, Pitch, number of scans and scan length. These parameters should be optimized for each specific examination (Rehani et al. 2007).

The tube kVp kilo voltage peak considered as the quantitative and qualitative radiation parameter. Thus, the intensity of X-ray beam depends on the kVp as it is proportional to the square of kVp. That means the image noise and radiation dose can be affected by any slight changes in kVp. Though tube output falls as kVp falls, the penetration through the body also falls and so the effect of changes to kVp will depend upon the body size being imaged. The tube current mAs the second significant parameter affect the radiation dose and the mage quality. The radiation dose is directly related to mAs. As a result, the radiation dose will decrease as the mAs decreased. However, the image noise is inversely proportional to the square root of the mAs. Pitch is also other important scanning parameters

as it depends on the tube collimation and table feed. If the scanning table moves faster relative to the tube rotation time then in that case pitch will increase and exposure time will decrease thus reducing dose to patient. Although, quick moving of a scanning table, it will affect the image quality by producing a certain image artefacts (Rehani et al. 2007).

3.6 Methods of optimising radiation dose in CT

Recently, radiologists and physicist focusing in the reduction of CT dose in SPECT/CT procedures. Taking into account that both exposure parameters and scan protocols contribute to a reasonable equality between the radiation exposure dose, image quality and other CT factors such as overall scanning time.

Several methods are available to optimise and minimise the radiation absorbed dose in CT. as founded in previous studies: justification, shielding of organs, modification of exposure parameters, limitation of scan length, use of anatomy-adapted tube current modulation, filtration, diagnostic reference levels, iterative image reconstruction methods and changing kV (Rehani et al. 2007).

In this project our methods used to optimise the scanning protocols by adjusting the scan parameters: tube voltage kVp, tube current mAs and pitch that is table travel per rotation.

Chapter 4

Methods

Phase l

4.1 Phantom Preparation

Objectives

As it is not ethical to apply an optimisation of X-ray CT dose within SPECT/CT protocols directly to patients, a phantom SPECT/CT study has been performed.

Description

An anthropomorphic torso phantom was used model ECT/TOR/P. It consists of a large body shaped cylinder with heart, lung, liver and the spine had been inserted (DSC, 2013). Likewise, the lung inserts can be filled with Styrofoam beads and water to simulate lung tissue density. Preparation of phantom had been divided into two parts. First of all, at St Georges Hospital, in Nuclear Medicine department a series of lumbar spine L1-L5 has been prepared, each vertebrae has been stabilised by a blue tack and the facet joints as well as shown in (*fig 4.1*). Then, that lumbar spine has been fitted into the phantom and taped by using a waterproof tape to make sure that they will not be floating in the water. Next, the phantom has been filled with water and has kept all the night to allow the bones absorb the water (*fig 4.2*).

4.2 Image Acquisition

The experiment were carried out at St Helier Hospital, Nuclear Medicine department, while reconstruction and image processing had been taken place in the workstation of the department. In this study the data have been obtained from a dual-headed SPECT with an integrated 6-slice CT scanner (Symbia T6, Siemens Medical Systems, Erlangen, Germany). The phantom had been positioned in the scanner table in the same position of a real patient during the diagnostic image acquisition i.e. head up position. Also, it had been stabilised by using a 10cc syringe as a wedge to prevent it from any slight movement during the scan. For

each acquisition the CT was acquired immediately after SPECT; the phantom was being kept in the same position to minimise offsets due to movement (*fig 4.3*).

Initially, the reference acquisition had been acquired by using the following CT parameters: tube current of 80 mAs, tube voltage of 100 kVp and pitch of 0.5 (*fig 4.4*), the CTDI_{vol} and the effective mAs had been recorded. After that, 11 different acquisitions had been acquired with different values of CT parameters and the CTDI_{vol} and the effective mAs had been recorded each time.

Fig 4.1: Lumbar Spine

Fig 4.2: Phantom's Preparation

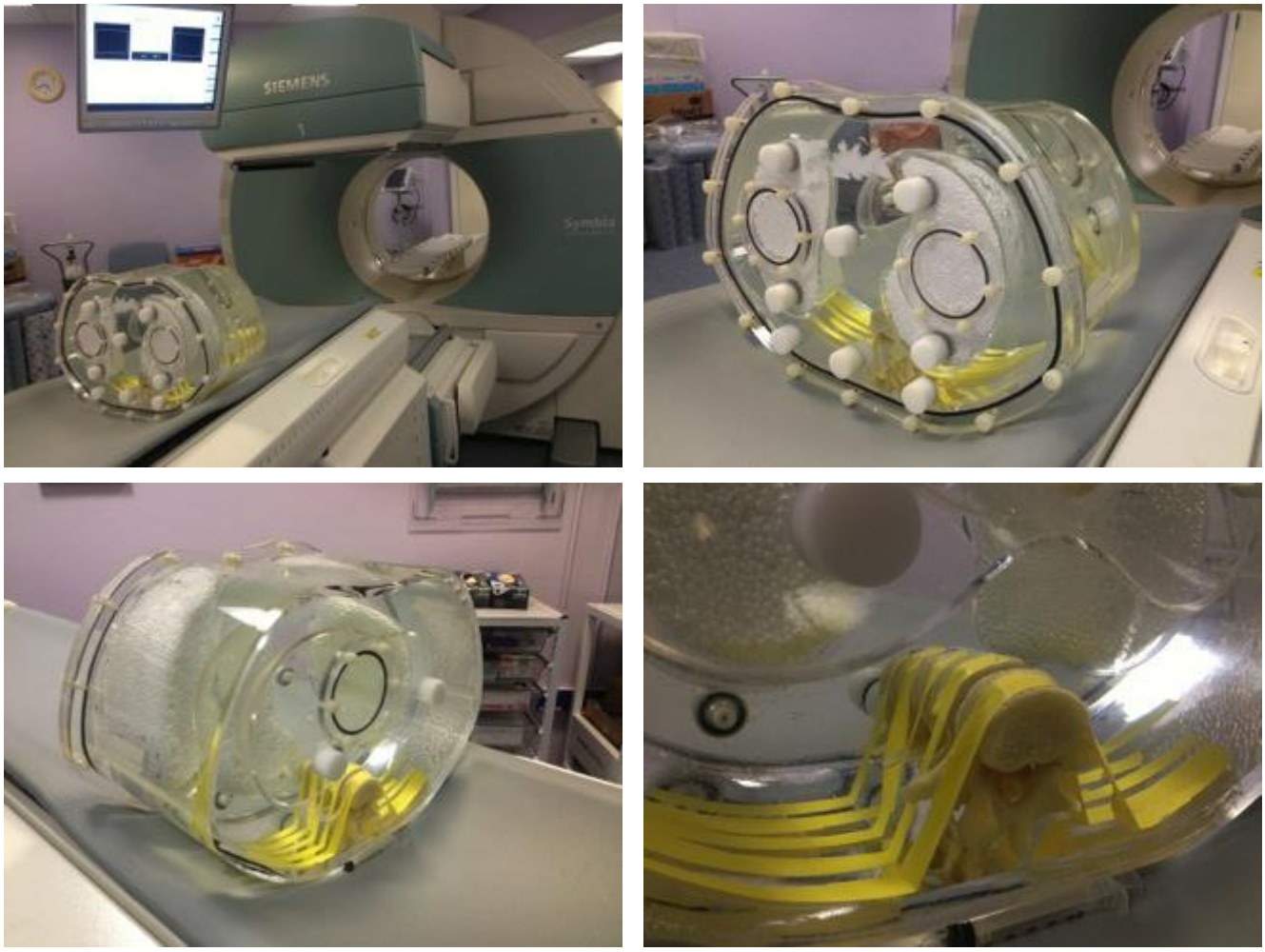

Fig 4.3: Phantom's Position

Fig 4.4: The Phantom and camera prepared for SPECT/CT study

Phase ll

4.3 Radioactivity administration

In the second part of the experiment the radioactivity source Tc^{99m} had been prepared. Preparation of the source had been in the hot lab of the nuclear medicine department at St. Helier Hospital. Two sources prepared to be administered into both sides of the facet joint. Moreover, a source in a syringe had been also prepared to be located alongside the lumbar spine. The reason why doing that is because of the need for a uniform area to measure the noise. Since the noise is very difficult to assess in non-uniform area i.e. facet joint. Though by inserting a syringe alongside the lumbar spine the attenuation correction resulted from construction will be uniform and CT slices will be uniform as well. So there is a possibility to read out the noise in the image (*fig 5.1*). Amounts of activity withdrawn are shown in the table below:

31st July	Tc^{99m}
In 0.1 ml	115.1 MBq
Facet Source 1	10.4 MBq At 10:11 AM
Facet Source 2	9.7 MBq At 10:13 AM
Syringe **In 12 ml**	23 MBq At 10:36 AM

Table 1: Amount of radioactivity withdrawn

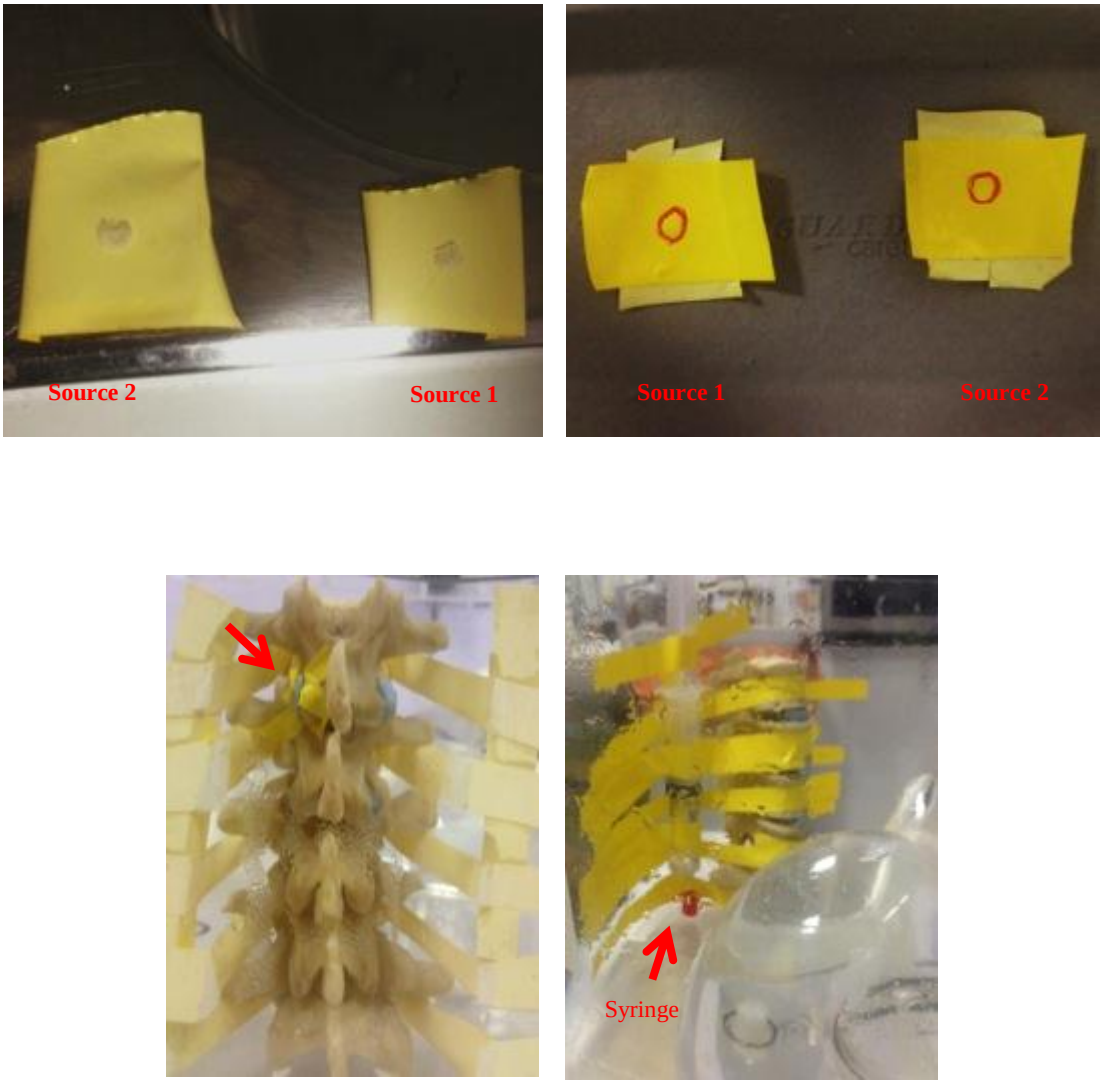

Fig 5.1: Preparation of radioactivity source

4.4 Image Acquisition

In order to get an accurate SPECT acquisition that is nearly similar to that acquisition acquired clinically on a real patient, a region of interest ROI drawing had been obtained on a previous clinical molecular images. That would be helpful in measuring the counts on nuclear image so that we can adjust our acquisition time to achieve the same clinical counts. By doing that we can correlate our phantom study results to be applied to a clinical study.

Firstly, from the previous clinical nuclear images a region of interest had been drawn around the pelvis and the total counts had been measured 10 times, and then the average had been calculated. Furthermore, from the SPECT protocol that has been used in St. Helier Hospital the time per frame is 8 sce. By dividing the average counts over 8, then the obtained number corresponds to the clinical counts/sec/frame. Next, from the patient positioning monitor PPM screen the rate of counts released from the phantom was 2.5 kcounts. Therefore, the total time required for the first acquisition was 11s (Appendix 3). The main purpose of that is to correlate the counts detected clinically with counts detected from the phantom so that the phantom study performed looks like the real clinical study.

In this part of the experiment three acquisitions had been acquired by using a constant high kVp 130, pitch 0.5 and varying the mAs 20, 40, 60 respectively. The first SPECT images had been taken and the acquisition had been started at 11:30 AM and the total time for frame/view was 11s. Then the CT had been acquired and the CTDI_{vol} and the effective mAs had been recorded. The image acquisition time for each SPECT frame was increased to account for radioactive decay, and to produce SPECT studies with equivalent counts. For example, the second SPECT images had been obtained at 11:55 AM with a total time for frame/view of 12 sec.

4.5 Images Analysis

Visual Assessment

After acquiring the whole 15 images we anonymised the images and hid the CT parameters, which is used in each acquisition. The reason why doing that is to display the images to the nuclear medicine radiologist so that he can evaluate the images qualitatively to decide weather it is acceptable or not. His decision was made according to several standards, which he is used to diagnose the clinical images in real patients. Those criteria are: Noise level in bones, Noise level in soft tissue, Spatial resolution, Clarity of the margins, Clarity of bone's detail in facet joint, Differences between cortical bone and medulla, Differences between cortical surface and soft tissue, Trabecular pattern in the medulla and Localization. We formulate those criteria in a table and ask the radiologist to rank the images (Appendix 5).

Noise from ROI

Statistical image noise was assessed of the last three acquisitions, which were acquired following the administration of radioactive material used with high kVp 130. A region of interest ROI was drawn within the syringe on the attenuation corrected SPECT image and also another ROI was drawn near to the spine in the CT image. CT noise was determined by readings standard deviation of CT numbers in each ROI.

Chapter 5

Results

5.1 Phase l

Reference

kVp	mAs	Pitch	$CTDI_{vol}$ mGy	Effective mAs
110	80	0.5	11.64	164

After the SPECT and CT acquisitions had been completed, the $CTDI_{vol}$ and effective mAs were recorded. The standard CT protocol, which is used at St Helier Hospital, is acquired firstly and considered as the starting point to read out the $CTDI_{vol}$, which is currently used in clinical lumbar spine patient studies, which is 11.64 mGy. So that we can compare that dose with the later doses delivered by the different acquisitions when we change the other CT parameters.

Acquisition l

kVp	mAs	Pitch	$CTDI_{vol}$ mGy	Effective mAs
110	80	1.0	12.21	172
110	80	1.5	10.93	154
110	80	1.8	11.0	155

Using constant kVp 110, mAs 80 and changing the pitch 1.0, 1.5, 1.8 respectively. Increasing the pitch value by 0.5 and we figured out that the maximum value that the CT machine can reached is 1.8. As mentioned previously, we expected that by increasing pitch it would lead to reducing the radiation dose. However, in our acquisition we found that the $CTDI_{vol}$ did not vary with pitch. That is due to the system itself, which alter the mAs automatically to keep the same image quality that is to keep the image noise approximately constant as pitch altered.

Acquisition ll

kVp	mAs	Pitch	$\mathbf{CTDI_{vol}}$ mGy	Effective mAs
80	80	0.5	6.96	240
130	80	0.5	16.79	154

Here, constant mAs 80, pitch 0.5 used with kVp 80, and 130. Varying the kVp value by using the lowest and highest values 80 and 130 respectively. As stated earlier there is a direct relationship between the kVp and the radiation to the patients. Then in our experiment there are significant alterations of $CTDI_{vol}$, which decrease and increase as the kVp changed. This alterations changed by a factor of 0.41.

Acquisition lll

kVp	mAs	Pitch	$\mathbf{CTDI_{vol}}$ mGy	Effective mAs
110	60	0.5	9.37	132
110	40	0.5	6.67	94
110	20	0.5	4.26	60

Constant kVp 110 and 0.5 pitch with change in mAs values 60, 40 and 20. Alteration of mAs with a standard kVp 110. Also the mAs is directly proportional to the radiation exposure dose. Here we observed that there was a decrease in $CTDI_{vol}$ as the mAs decreased by a factor of 3. It was surprisingly noted that the reduction of the reported CTDI dose was only by a factor of 2.2.

Acquisition lV

kVp	mAs	Pitch	$CTDI_{vol}$ mGy	Effective mAs
80	60	0.5	4.81	166
80	40	0.5	3.42	118
80	20	0.5	2.03	70

Low kVp 80 and 0.5 pitch with change in mAs values 60, 40 and 20. Alteration of mAs with a low kVp 80. Similarly, we notice that the $CTDI_{vol}$ decreased, though only by a factor of 2.36 and not 3 as expected from the mAs change.

5.2 Phase ll

Acquisition V

kVp	mAs	Pitch	$CTDI_{vol}$ mGy	Effective mAs
130	60	0.5	13.08	120
130	40	0.5	9.16	84
130	20	0.5	5.89	54

High kVp 130 and 0.5 pitch with change in mAs values 60, 40 and 20. In order to get an accurate SPECT acquisition which is nearly correspond to the clinical one we use the decay equation $I = I_0\, e^{-\lambda t}$ to calculate the actual time per frame (Appendix 4). The SPECT/CT acquisition parameters used per detector are as follows: 180° configuration, 180° rotation, 64 views, non-circular orbit and Low Energy High Resolution LEHR collimator. In this phase firstly we acquire the SPECT as the radioactive material had been administered. After that the SPECT image is reconstructed automatically by the system. The reconstruction parameters used are as follows: Flash 3D, number of subset 4, 8 Iterations, 8.4 mm Gaussian filter. Then the CT image acquired by using high kVp 130 with alteration in mAs values 60, 40 and 20 consequently. The $CTDI_{vol}$ decreased by a factor of 2.22.

5.3 Images Analysis

Protocol		Acceptable	Non-acceptable	$CTDI_{vol}$ mGy	Noise (SD)	
					CT	Attenuation Corrected SPECT
A	Reference: 110 kVp 80 mAs 0.5 Pitch	6	2	11.64		
B	110 kVp 80 mAs 1.0 Pitch	7	1	12.21		
C	110 kVp 80 mAs 1.5 Pitch	7	1	10.93		
D	110 kVp 80 mAs 1.8 Pitch	7	1	11.0		
E	80 kVp 80 mAs 0.5 Pitch	5	3	6.96		
F	130 kVp 80 mAs 0.5 Pitch	5	3	16.79		
G	110 kVp 60 mAs 0.5 Pitch	7	1	9.37		
H	110 kVp 40 mAs 0.5 Pitch	3	5	6.67		
I	110 kVp 20 mAs 0.5 Pitch	5	3	4.26		
J	80 kVp 60 mAs 0.5 Pitch	1	7	4.81		
K	80 kVp 40 mAs 0.5 Pitch	0	8	3.42		
L	80 kVp 20 mAs 0.5 Pitch	0	8	2.03		
M	130 kVp 60 mAs 0.5 Pitch	8	0	13.08	69.64	62.07
N	130 kVp 40 mAs 0.5 Pitch	6	2	9.16	54.67	56.67
O	130 kVp 20 mAs 0.5 Pitch	5	3	5.89	67.37	59.48

Table 2: The results of the images acquired

After anonymising the images and hiding the CT parameters, the images from 1 to 15 displayed to the radiologist to analyse them and decide whether it is acceptable or not according to the interpretation criteria. The table above shows the radiologist's analysis he decided that two of them are not acceptable which are ***K*** and ***L*** and those images correspond to low kVp 80 with low mAs 40 and 20 respectively. The most acceptable one is ***M*** and the CT parameters used are high kVp 130 and 60 mAs. The most images he considered them nearly acceptable which are ***B***, ***C***, ***D*** which are acquired with alterations of pitch and that is expected because the alteration of pitch did not change the image quality. Also image ***G*** is almost acceptable and its parameters are nearly the parameters used for the reference 110 kVp and 60 mAs. The rest images fluctuated between the acceptable and non-acceptable the table below shows the images in the order of most acceptable to least acceptable.

Protocol			Acceptable	Non-acceptable	$CTDI_{vol}$ mGy	Noise (SD)	
						CT	Attenuation Corrected SPECT
1	**M**	130 kVp 60 mAs 0.5 Pitch	8	0	13.08	69.64	62.07
2	**B**	110 kVp 80 mAs 1.0 Pitch	7	1	12.21		
3	**C**	110 kVp 80 mAs 1.5 Pitch	7	1	10.93		
4	**D**	110 kVp 80 mAs 1.8 Pitch	7	1	11.0		
5	**G**	110 kVp 60 mAs 0.5 Pitch	7	1	9.37		
6	**A**	Reference: 110 kVp 80 mAs 0.5 Pitch	6	2	11.64		
7	**N**	130 kVp 40 mAs 0.5 Pitch	6	2	9.16	54.67	56.67
8	**E**	80 kVp 80 mAs 0.5 Pitch	5	3	6.96		
9	**F**	130 kVp 80 mAs 0.5 Pitch	5	3	16.79		
10	**I**	110 kVp 20 mAs 0.5 Pitch	5	3	4.26		
11	**O**	130 kVp 20 mAs 0.5 Pitch	5	3	5.89	67.37	59.48
12	**H**	110 kVp 40 mAs 0.5 Pitch	3	5	6.67		
13	**J**	80 kVp 60 mAs 0.5 Pitch	1	7	4.81		
14	**K**	80 kVp 40 mAs 0.5 Pitch	0	8	3.42		
15	**L**	80 kVp 20 mAs 0.5 Pitch	0	8	2.03		

Table 3: The results of the images acquired ordered from most acceptable to least acceptable

Unfortunately, the radiologist could not be able to rate the images according to localisation. That is because we faced a technical problem in the system which unable us to display the fused images of SPECT with CT. After scaling the images I asked the radiologist to rate them from 1 to 15 according to the best. But he could not do that since it was impossible to display the whole 15 images in one screen. Instead he decided the best image in his point of view, which is ***M*** and the worst, which is ***L***. That matches his evaluation according to the 8th criteria. Image ***M*** corresponds to the image acquired with 60 mAs, 130 kVp. While image ***L*** corresponds to the image acquired with 20 mAs, 80 kVp. That coincides with the fact that higher kVp is used to increase the penetration in obese patients. Since our phantom sizes, which we used in the experiment, is for large patient. In regards to patient dose the $CTDI_{vol}$ decreased as decreasing the mAs, which also agrees with the fact that dose, is proportional to mAs.

Instead of rating the SPECT/CT images which is acquired by the administration of the radioactive material qualitatively. A region of interest ROI had been drawn around the syringe in the corrected image that is the attenuation corrected nuclear medicine counts and the spine in CT image (fig 6.1). Measurements of standard deviation had been made to determine the noise quantitatively as shown in the table below:

	Standard Deviation SD	
	CT	**Attenuation Corrected SPECT**
kVp 130, mAs 20	76.69	61.57
kVp 130, mAs 40	62.63	58.11
kVp 130, mAs 60	49.78	58.00

Table 4: SD of the CT image and attenuation corrected SPECT

It is known that noise is the standard deviation SD of pixel values that is measured inside a uniform area of interest in the image and it is expressed in terms of Hounsfield Unit (Primak et al., 2006). CT noise depends on several factors: the number of X-ray photons, which reach the detector that is quantum noise, detection efficiency, electronic noise and the reconstruction kernel. Quantum noise is proportional to $\sqrt{N}$ while the corresponding image noise is proportional to $1/\sqrt{N}$ where N is the number of photons that leads to the reconstructed image (Strack et al., 2002). To indicate the noise in CT, the SD is used to demonstrate the significance random fluctuation in the CT number. Thus the higher the SD is the greater the image noise (Goldman, 2007). In that case in our experiment the larger the CT image noise is the higher the kVp 130 and lower mAs 20 which is 76.69 in the CT image and 61.57 in the attenuation corrected SPECT image. The noise difference in the CT image between the highest and lowest mAs is given by 65 %. Also in the attenuation corrected SPECT image the image noise is vary by 94 %.

It is obvious that the radiologist prefer the image with the highest kVp, highest mAs and lowest image noise. We cannot consider that protocol is the best as the $CTDI_{vol}$ is higher which is 13.08 mGy. The following accepted acquisitions, which are depending on the variation of pitch only, could be considered the best protocol since the $CTDI_{vol}$ remains nearly the same as the $CTDI_{vol}$ of the reference ~ 11.00 $\pm$ 1.21 mGy. Also the acquisition that acquired with decreasing the mAs to 60 could be considered acceptable because the $CTDI_{vol}$ is reduced by factor of 1.24.

Attenuation Corrected SPECT **CT**

130 kVp 20 mAs

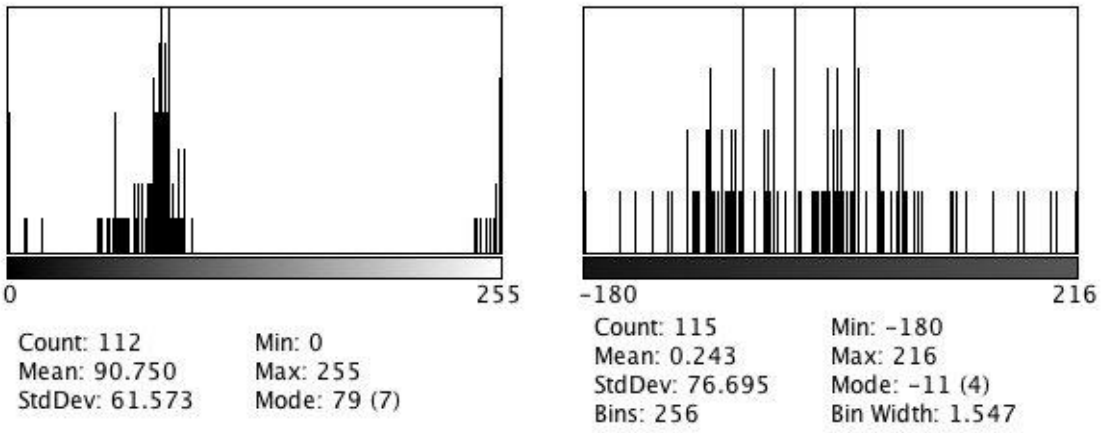

130 kVp 40 mAs

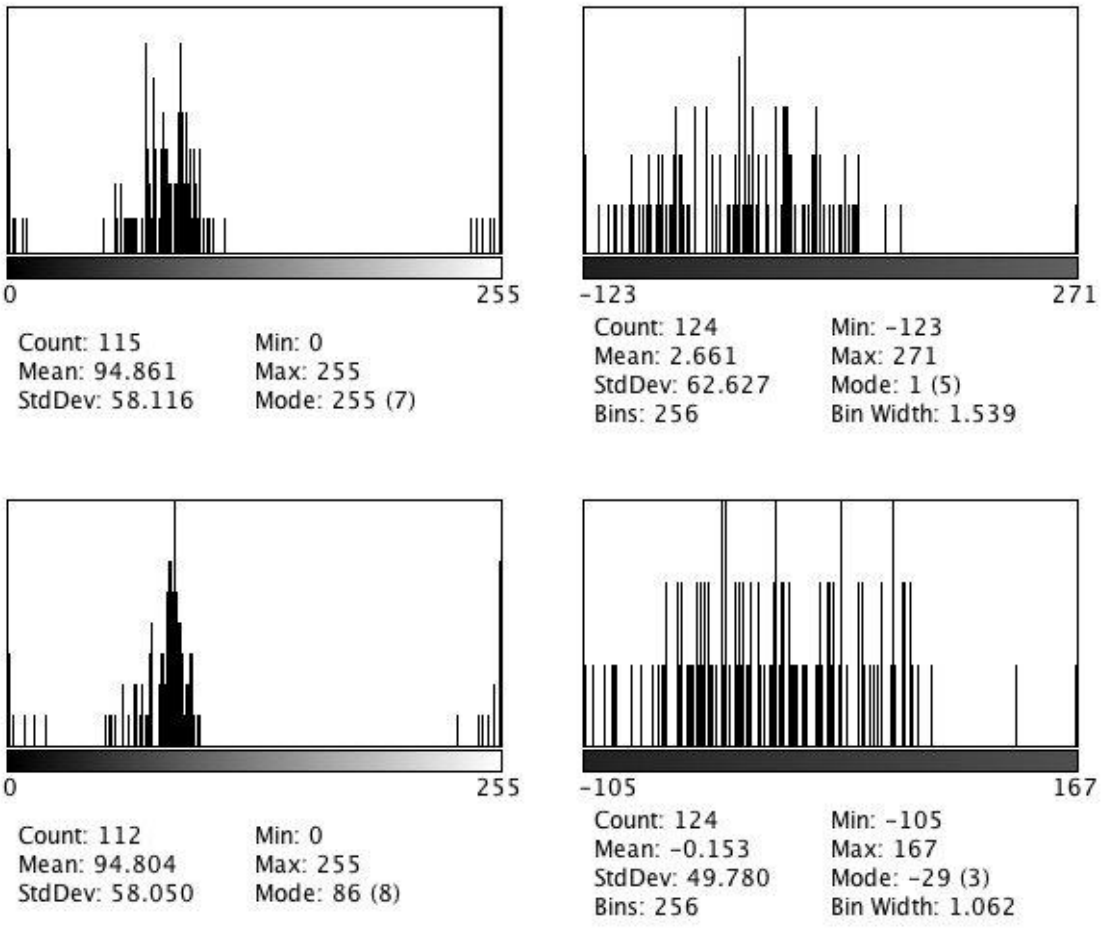

Fig 6.1: SD of the attenuation corrected SPECT images and CT images

Chapter 6

Discussion and Conclusions

The main goal in this project was to optimise the X-ray CT dose within SPECT/CT studies especially in lumbar scan facet joint (FJ) studies, for localisation not diagnostic CT imaging. It had been chosen since it is currently considered as such type of study need to be focused on at St. Helier Hospital. A number of acquisitions had been acquired with alteration of CT parameters that is kVp, mAs and pitch. The $CTDI_{vol}$ and effective mAs readings had been recorded. Finally, analysis of the acquired images had made qualitatively by a nuclear medicine radiologist and quantitatively by measuring the CT noise that is standard deviation. Analysis made for localisation purposes only. The final results could be applied for a large patient since our phantom size is corresponding to a large patient.

The best image obtained in a qualitative manner or by visual assessment that acquired with a high kVp 130 and 60 mAs. That is expected, as the large patient needs more radiation penetration and more number of photons detection. According to the quantitative assessment of the CT noise by measuring the standard deviation SD of the CT image we found that the higher the kVp 130 and higher mAs 60 is the lowest noise in the image by 65 %. The difference in $CTDI_{vol}$ between the reference image that is 110 kVp and 80 mAs and the best image quality decided by the radiologist which is 130 kVp and 60 mAs is given by a factor of 1.24 more with the high kVp. While the differences in the effective mAs is higher with 110 kVp by a factor of 1.36.

The best image quality could not be considered as the best protocol since our goal is to optimise the X-ray CT dose and that protocol expose the patients with higher doses. That means we have to reach a reasonable CT dose can be exposed to patients and at the same time obtaining a good image for localisation purposes. According to the experiment all the images acquired with alteration in pitch gave an acceptable results in addition to reasonable $CTDI_{vol}$ doses. Also, the image acquired with lowering the mAs to 60 gave the same image results.

As the time period of my project was limited, I could not manage to figure out the problem with the workstation system at St. Helier Hospital to display the integrated CT and SPECT images to evaluate them according to localisation. For further work recommendations it is important to pay an attention during acquiring the SPECT images and make sure that the counts detected is suitable and correspond to the clinical counts so that the display of the

image fusion of SPECT with CT would be possible. Also, it would be better to check that the save screen image displays the anatomy and the molecular image correctly which allows us to review the image in case that the fusion display is not work successfully. Follows that the radiologist can be able to read the images and evaluate the localisation. Finally, it is important to have some clinical images as an example so that we can correlate the phantom study to the clinical one. Also the decision of whether the images are acceptable or not could be made easier with existing of a previous study so that we can use it as a reference protocol.

Appendices

Appendix [1]

Bone Scan SPECT/CT

No.	Height M	Height^2 m^2	Weight Kg	BMI	Thickness cm	kVp	mAs	CTDI$_{vol}$ mGy
1	1.60	2.56	46.95	18.34	21.44	110	90	9.39
2	1.70	2.89	61.00	21.11	24.17	110	128	9.09
3	1.63	2.66	57.00	21.45	19.73	110	126	8.95
4	1.57	2.46	58.90	23.90	21.85	110	138	9.80
5	1.78	3.17	76.90	24.27	23.06	110	134	9.00
6	1.73	2.99	76.00	25.39	23.76	110	190	13.49
7	1.60	2.56	71.20	27.81	24.54	110	182	12.92
8	1.90	3.61	102.00	28.25	27.74	110	164	10.00
9	1.77	3.13	92.45	29.51	28.25	110	166	11.79

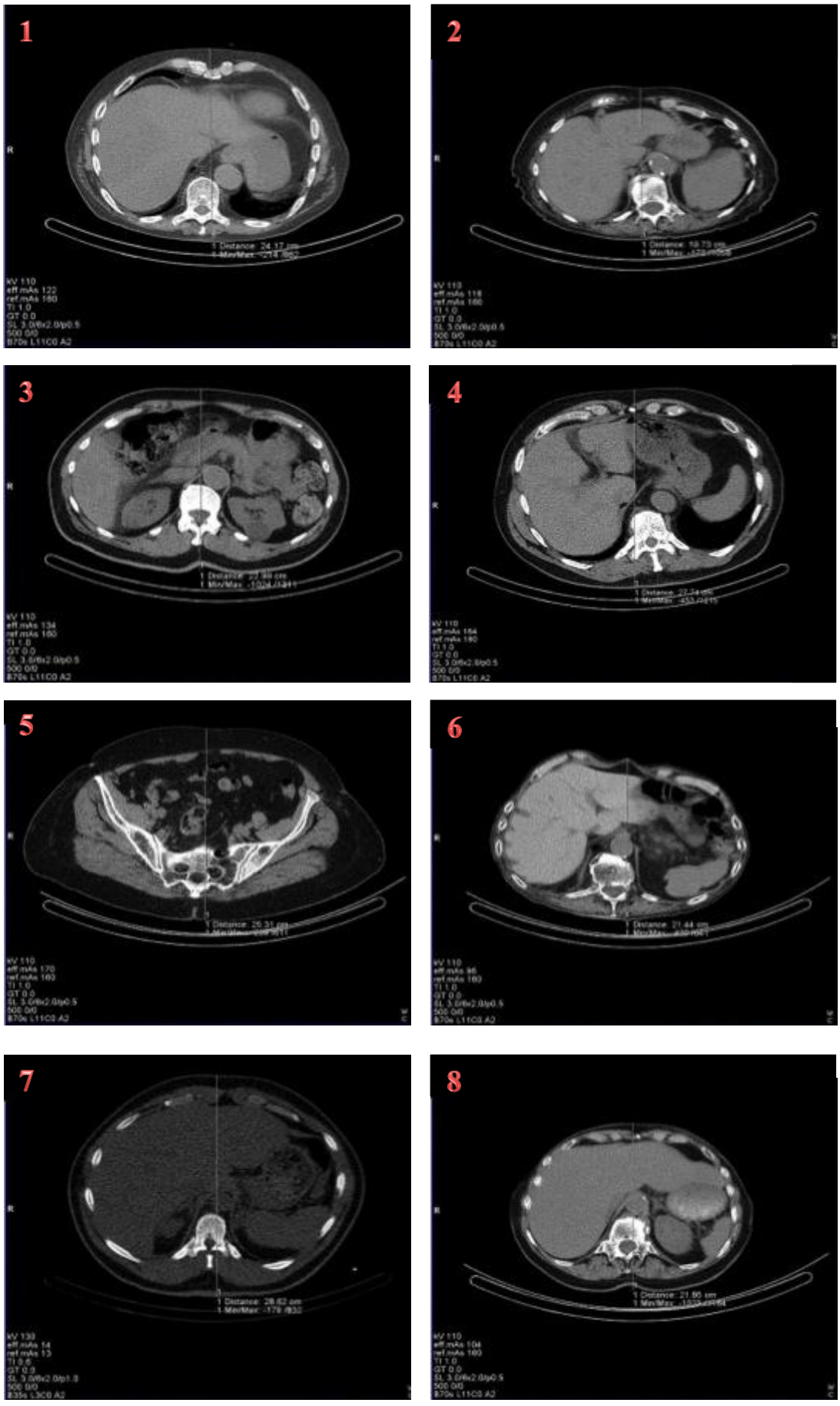

Examples of Bone Scan: Abdominal cross sectional image dimensions

Appendix [2]

Cardiac Scan SPECT/CT

No.	Height m	Height^2 m^2	Weight Kg	BMI	Thickness cm	kVp	mAs	CTDI$_{vol}$ mGy
1	1.68	2.82	60.00	21.26	20.61	130	14	1.22
2	1.75	3.06	67.00	21.88	23.55	130	13	1.37
3	1.63	2.66	70.00	26.35	24.79	130	13	1.37
4	1.57	2.46	76.00	30.83	25.92	130	16	1.83
5	1.52	2.31	74.00	32.03	27.38	130	13	1.57
6	1.55	2.40	78.00	32.47	27.79	130	13	1.44
7	1.80	3.24	110.00	33.95	29.86	130	13	2.35
8	1.88	3.53	127.00	35.93	37.71	130	25	2.75
9	1.87	3.50	127.00	36.32	37.71	130	17	1.90

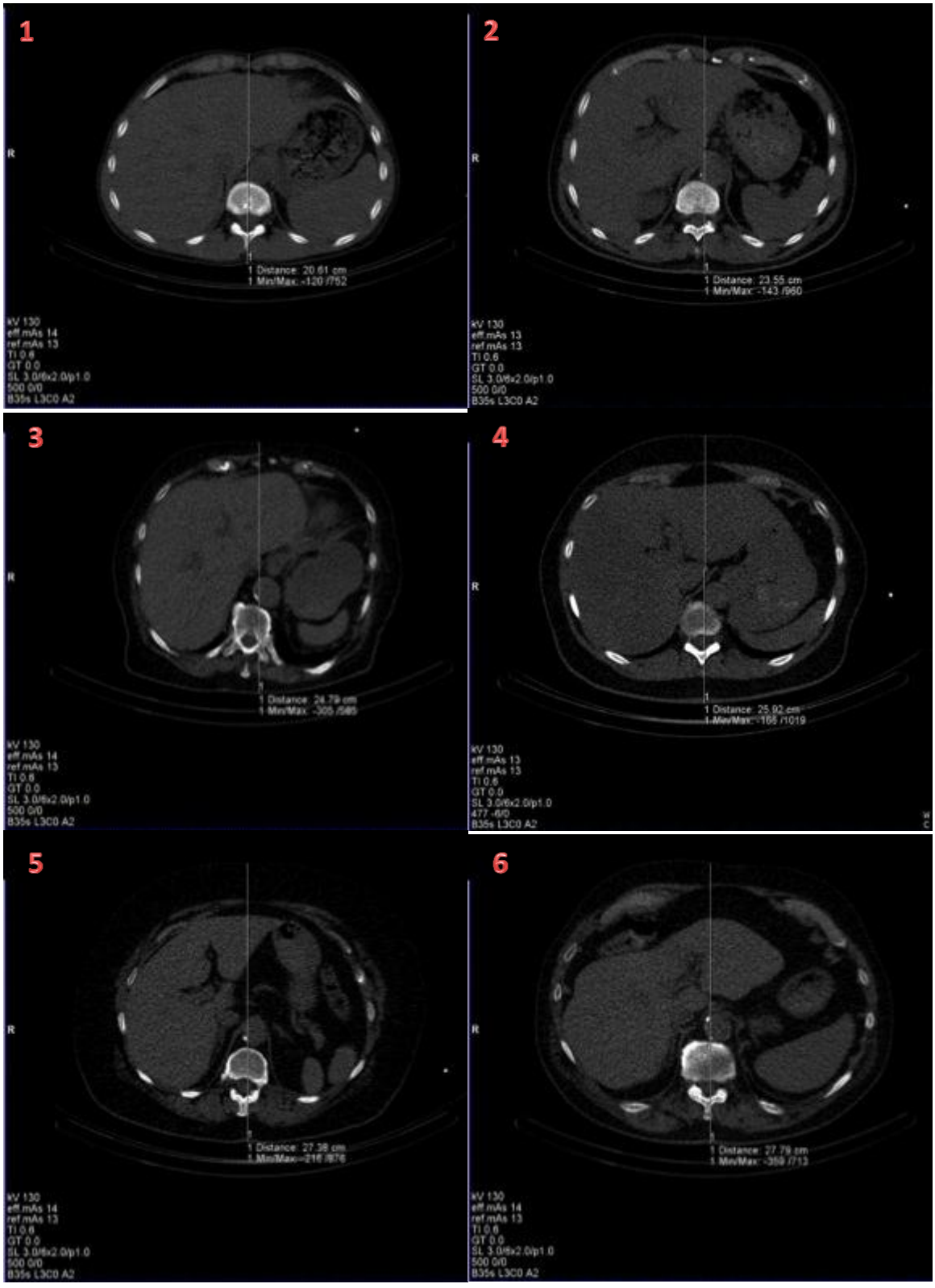

Examples of Cardiac Scan: Abdominal cross sectional image dimensions

Appendix [3]

Frames	Clinical counts per frame
1	226288
2	237275
3	242774
4	240439
5	231576
6	222202
7	214589
8	204765
9	194889
10	219068
Average	223386.5
Clinical time per frame	8 sec/view
Clinical Counts/frame/sec	27923 Counts/s/frame
Clinical Kcounts /frame/ sec	28 Kcounts/s/frame
Phantom PPM count rate	2.5 Kcounts/s/frame
Phantom scan time per view	11 sec

Appendix [4]

Acquisition	Scanning Time 31/07/2013	Time per frame (s)
60 mAs, 130 kVp	11:30 AM	11
40 mAs, 130 kVp	11:55 AM	12
20 mAs, 130 kVp	12:20 AM	12

Appendix [5]

No.	Criteria	Scale	
		Acceptable	Non Acceptable
1	Noise level in bones		
2	Noise level in soft tissue		
3	Spatial resolution		
4	Clarity of the margins		
5	Clarity of bone's detail in facet joint		
6	Differences between cortical bone and medulla		
7	Differences between cortical surface and soft tissue		
8	Trabecular pattern in the medulla		
9	Localization		
Total			

References

Bongartz, G. Golding, S. Jurik, A. Leonardi, E. van Persijn van Meerten, E. et al. (2004). **European Guidelines for Multislice Computed Tomography**. The 2004 CT quality criteria. Appendix A: MSCT dosimetry..

Carstensen, M. Alharbi, M. Urbain, J. Belhocine, T. **SPECT/CT Imaging of the Lumbar Spine in Chronic Low Back Pain: a case report**. Chiropractic & Manual Therapies, 19(2), 2011.

Data Spectrum Corporation DSC, **Anthropomorphic Torso Phantom** [online]. Available from; www.spect.com/pub/**Anthropomorphic_Torso_Phantom**.pdf [Accessed 9 Aug 2013].

De Maeseneer, M. Lenchik, L. Everaert, H. Marcelis, S. Bossuyt, A. Osteaux, M. Beeckman, P. **Evaluation of Lower Back Pain with Bone Scintigraphy and SPECT**. Radiographics, 19(4): 901-12, 1999.

David J. Dowsett, Patrick A. Kenny and R. Eugene Johnston, **The Physics of Diagnostic Imaging**, 2nd ed. London: Hodder Arnold, 2006.

Delbeke, D. Schoder, H. Martin, W. Wahl, R, **Hybrid Imaging (SPECT/CT and PET/CT): Improving Therapeutic Decisions**. Seminars in Nuclear Medicine, 39(5): 308-340, 2009.

Eugene C. Lin, **Radiation Risk from Medical Imaging**. Mayo Clinic Proceedings, 85 (12): 1142-1146, 2010.

eMED TV Health information brought to life, **How to Calculate BMI** [online]. Available from: http://bmi.emedtv.com/bmi/how-to-calculate-bmi.html [Accessed 22 July 2013].

Goldman, L. **Principles of CT: Radiation Dose and Image Quality**. Journal of Nuclear Medicine Technology, 35(4): 115-128, 2007.

Hsieh, J. **Computed Tomography: Principles, Design, Artifacts and Recent Advances**. USA: The International Society for Optical Engineering, 2013.

Hu, H. **Multi-slice helical CT: scan and reconstruction**. Medical physics, 26 (5), 1999.

Jacene, H. Geotze, S. Patel, H. Wahl, R. Ziessman, H, **Advantages of Hybrid SPECT/CT *vs* SPECT Alone**. The Open Medical Imaging Journal, 2: 67-69, 2008.

Kalra, M. Maher, M. Parasad, S. Hayat, M. Blake, M. Varghese, J. Halpern, E. Saini, S, **Correlation of Patient weight and Cross Sectional Dimensions with Subjective Image Quality at Standard Dose Abdominal CT**. Korean Journal of Radiology, 4(4): 234-238, 2003.

Kim, S. Song, H. Samei, E. Yin, F. Yoshizumi, T, **Computed Tomography Dose Index and Dose Length Product for Cone-Beam CT: Monte Carlo Simulations of a Commercial System**. Journal of Applied Clinical Medical Physics, 12(2), 2011.

Kopp, A. F., Klingenbeck-Regn, K., Heuschmid, M., Kuttner, A., Ohnesorge, B., Flohr, T., Schaller, S. & Claussen, C. D., **Multislice Computed Tomography: Basic Principles and Clinical Applications**. ELECTROMEDICA-ERLANGEN-, 68(2), 94-105, 2000.

Larkin, A. Serulle, Y. Wagner, S. Noz, M. and Friedman, K, **Quantifying the Increase in Radiation Exposure Associated with SPECT/CT Compared to SPECT Alone for Routine Nuclear Medicine Examinations**. International Journal of Molecular Imaging, vol. 2011, Article ID 897202, 5 pages, 2011. doi:10.1155/2011/897202

Maher K, et al., **Basic Physics of Nuclear Medicine**. Germany: Wikibooks, 2006.

Makki, D. Khazim, R. Zaidan, A. Ravi, K. Toma, T, **Single Photon Emission Computerized Tomography SPECT scan-positive Facet Joints and Other Spinal Structures in a Hospital-Wide Population with Spinal Pain**. The Spine Journal, 58-62, 2010

McCollough, C. Bruesewitz, M. Kofler, J, **CT Dose Reduction and Dose Management Tools: Overview of available Options**. Radiographics, 26(2): 503-512, 2006.

Mhiri, A. Slim, I. Ghezaiel, M. Slimene, M. **Estimation of Radiation Dosimetry for some common SPECT-CT Exams**. International Journal of Biotechnology for Wellness Industries, 1, 266-269, 2012.

O'Neill, C. Owens, DK, **Role of Single Photon Emission Computed Tomography in The Diagnosis of Chronic Low Back Pain**. Spine Journal, 10(1): 70-72, 2010.

Powsner R.A., Powsner E.R. **Essential Nuclear Medicine Physics**, 2nd ed. UK: Blackwell, 2006.

Primak, A. McCollough, C. Bruesewitz, M. Zhang, J. Fletcher, J, **Relationship beween Noise, Dose and Pitch in Cardiac Multi Detector Row CT**. Radiograpjics, 26(6): 1785-1794, 2006.

Pryor, M. (2013) **Quality Management and Radiation Protection**. University of Surrey, Guildford, 8 February 2013. Guildford: Royal Surrey County Hospital.

Rehani, M. Tsapaki, V. **Dose Management in CT Facility**. Biomedical Imaging and Intervention Journal, 3(2): e43, 2007.

Schutz, U. Cakir, B. Deinhofer, K. Richter, M. Koepp, H. **Diagnostic value of Lumbar Facet Joint Injection: A prospective Triple Cross-Over Study**. A Peer-Reviewed Open Access Journal, 6(11): e27991, 2011.

Sharma, P. Sharma, S. Ballal, S. Bal, C. Malhotra, A. Kumar, R. **SPECT-CT in routine clinical practice: increase in patient radiation dose comared with SPECT alone**. Nuclear Medicine Communications, 33(9): 926-32, 2012.

Sharp, P. Gemmell, H. Murray, A. **Practical Nuclear Medicine**, 3rd ed. London: Springer, 2005.

Siemens, **Computed Tomography its History and Technology** [online]. Available from:http://www.medical.siemens.com/siemens/zh_CN/gg_ct_FBAs/files/brochures/CT_History_and_Technology.pdf [Accessed 1 July 2013].

Soderberg, M, **Image Quality Optimisation and Dose Management in CT, SPECT/CT and PET/CT.** PhD thesis, Lund University, 2012.

Stabin, M. Tagesson, M. Thomas, S. Ljungberg, M. Strand, S, **Radiation Dosimetry in Nuclear Medicine.** Applied Radiation and Isotopes, 50: 73-87, 1999.

Strack, G. Lonn, L. Cederblad, A. Forssellaronsson, E. Sjostrom, L. Alpsten, M. **A Methods to Obtain the Same Levels of CT image Noise for Patients of Various Sizes to Minimise Radiation Dose**. The British Journal of Radiology, 75: 140-150, 2002.

Thompson, J. Tootell, A. Driver, J. Griffiths, M. Kane, T. Szczepura, K. Holmes, K. Mountain, V. Hogg, P, **Focusing in on SPECT-CT**. Society & College of Radiographers, 26-30, 2009.

Walker, P. (2013) **Detection and Dosimetry of Ionising Radiation**. University of Surrey, Guildford.